ELECTROMAGNETIC SUBSURFACE IMAGING. A CASE FOR AN ADAPTIVE BORN APPROXIMATION

NIELS B. CHRISTENSEN
Department of Earth Sciences, Aarhus University, Denmark

Abstract. The process of interpretation of electromagnetic data has many facets of which fast approximate interpretation techniques is an intriguing one. A new variant of the Born approximation – the Adaptive Born approximation – is presented and exemplified through 1D and 2D imaging techniques for transient electromagnetic data. The Adaptive Born approximation is generally applicable in approximate inversion schemes for inductive electromagnetic data as a one-pass imaging algorithm. Though it is as simple to use as the ordinary Born approximation, it offers a more accurate inverse mapping.

In the first part of this paper an attempt will be made to give an overview of fundamental concepts in electromagnetic subsurface imaging relevant for approximate inverse mappings and to outline major trends in present day modeling and inversion of electromagnetic data. This is of course an impossible task – certainly for this author – and much important work will not be mentioned in the limited space of the following. My apologies to the people who are not mentioned and whose research is not given credit here though it should have been. Naturally, my choice of references reflects the "schools" and circles I have been subjected to, but I hope that the list of references to developments in electromagnetic methods will point to papers of importance and thereby to other references for the interested reader.

Key words: electromagnetic, modeling, inversion, imaging, transient electromagnetic method

1. Introduction

1.1. IMAGING

The term imaging has been used in many different contexts in geophysics. Sometimes it is used to generally indicate interpretation of geophysical data. However, I think the term should be reserved for fast approximate ways of interpretation of data, so imaging could be defined as "an approximate inverse mapping of data into a model".

The concept of imaging is central in geophysics as in any science. Imaging means to produce a picture or a conceptual model of something. It is no coincidence that the term refers to the visual sense which is the one through which humans are capable of handling and sorting the largest amount of information. Seeing is believing, and a picture is worth a thousand words, to quote a few bon mots. Long rows of numbers do not produce the same qualitative understanding as curves, plots, contoured maps of certain parameters, model sections, depth slices, etc.

In electromagnetic methods in geophysics there are many levels of imaging. The most simple kind is the transformation of data into an apparent resistivity or

Surveys in Geophysics **18:** 477–510, 1997.

conductivity curve which will give a qualitative understanding of basic characteristics of the subsurface conductivity distribution. Beyond the level of mere data transformation there are a number of imaging methods which rapidly will give an approximate interpretation of the data set. These methods are important for in-field processing and they make it possible to change data recording strategies while measuring. Many of these methods are based on a one-dimensional (1D) earth model and must necessarily be fast. On a still higher level we find the methods which involve a 2D or 3D earth model, but which are still so fast, that they can be applied to large data sets as a standard processing procedure. Though slower than the simple 1D methods their advantage is the removal of the lateral effects of 1D imaging of data recorded over 2D and 3D structures. These methods serve to identify the subsets of the data volume where interesting anomalies are present and where rigorous but much more time consuming inversion procedures should be used.

To understand imaging in the context of interpretation of electromagnetic data, let us look at some basic concepts of electromagnetic methods in applied geophysics

1.2. RESOLUTION

The propagation of electromagnetic fields through the subsurface is governed by the Maxwell equations (Ward and Hohmann 1987). These equations describe all electromagnetic phenomena through three material constants: the magnetic permeability μ, the electrical conductivity σ, and the electrical permittivity ϵ. Most electromagnetic methods of applied geophysics make use of signals with frequencies, ω, so low that $\sigma \gg \omega\epsilon$ for most earth materials, and so conduction currents dominate over polarization currents. This means that the quasi-static approximation to the Maxwell equations can be used. For most geologic materials the magnetic permeability does not vary much, and so for most electromagnetic methods the electrical conductivity σ is the governing parameter. This means that the propagation of electromagnetic fields is described by the diffusion equation. This accounts for the inherent lack of resolution of electromagnetic measurements.

Our most immediate personal experience with a physical phenomenon described by the diffusion equation is the conduction of heat through solids, e.g. our own bodies, and with this picture in mind of the unfocussed and passive nature of the conduction of heat, it is easy to understand why electromagnetic methods have so poor resolution capabilities as is the case. It is very difficult to hold someone's hand to warm just the index finger. The whole hand – at least – tends to get warm.

High frequency methods like radar and photometry in the visible frequency spectrum are governed by the wave equation and thus have a much better resolution. However, with increasing conductivity the attenuation of the fields increases, and often earth materials have a conductivity which precludes the use of high frequency methods for investigations to depths exceeding a few meters. The whole field of georadar shall not be mentioned further in this paper.

In recent years very early-time transient equipment (VETEM) and high frequency sounding equipment have been under development (Pellerin et al. 1994, 1995; Stewart et al. 1994; Anderson 1995) in which frequencies above 10 MHz are used. For such measurements both diffusion and wave propagation is involved and both must be taken into account.

1.3. Complexity and description

Those of us occasionally digging the garden would probably agree that nature is a mess. All sorts of matter with very different properties are jumbled together to form our back yard. And the problem is not confined to the scale of a shovel. Many outcropping rocks look as if they were put together from whatever bits and pieces were at hand, which is exactly what they were, I suppose. The world is inhomogeneous, anisotropic, displays both slow and abrupt changes, and is – fortunately – full of surprises, and behind any of our attempts to harness nature in scientific descriptions is the unruled and basically indescribable complexity of the universe.

Though physical laws are believed to fully describe natural phenomena in all their complexity (until otherwise proved), the question of numerical solutions and computations puts a practical limit to the degree of complexity with which we can quantitatively describe natural phenomena. We are forced to adopt a simplified model of nature. The history of the development of electromagnetic geophysical methods is the history of the increasing complexity of the models with which we try to describe – at least – the major features of the subsurface.

Two aspects are of major importance when the level of complexity of a physical model is considered: its computability and its relevance. This means that the model must be simple enough that responses can be calculated within a reasonable time with the numerical methods at hand, yet complex enough to adequately describe the features of nature in which we are interested. Due to the complexity of electromagnetic phenomena the geophysical models which have lent themselves to computation have for a long time been quite inadequate to describe the complexities seen in the collected data, but simple models have nevertheless served their purpose well in illustrating fundamental characteristics of electromagnetic phenomena.

With the development of powerful modeling and inversion techniques through major improvements in computing speed and efficiency of programming codes another aspect of the modeling problem becomes increasingly important: the problem of relevance. There is no point in having a model with details which cannot be resolved by the measured data of the particular geophysical method used.

Electromagnetic geophysical data are – like all measurements of physical quantities – inaccurate, inconsistent and insufficient (Jackson 1972) for their purpose, i.e. for inferring the subsurface conductivity. Recorded data are inevitably sampled more or less sparsely in space and time and are thus aliased. Moreover, the detected

signal always contains noise. The computerization of electromagnetic field equipment and an inventive application of both analog and digital on-line processing has contributed significantly to the accuracy of measurements and noise reduction (Eaton and Hohmann 1987; Macnae et al. 1984; Becker and Cheng 1987) and improved the extremely important quality assessments of the recorded data. It is of primary importance for inversion of electromagnetic data that quantitative measures of the reliability of the data can be given.

With enhanced modeling and inversion capabilities more attention must be given to the fact that to justify the use of modern interpretation tools involving 2D and 3D models a densely measured data set over a considerable area is required. With the recent developments in interpretation tools there is in many ways a "measurement gap" between the data sets which can be interpreted – and which are required to justify the interpretation method – and the data sets actually recorded. Much effort should be – and is in fact – directed towards the development of cost-effective electromagnetic methods which will perform a much denser sampling in space and time of the measured field quantities. These methods will produce the more detailed and complex data sets, which demand – and justify – the use of more complex models of interpretation.

With airborne EM methods densely measured profiles have been recorded for some time and airborne methods are in rapid development as far as accuracy and the number of recorded field components are concerned. Also within the field of environmental geophysics modern efficient equipment has been invented and a few examples shall be given here. New continuous methods have been developed for geoelectrical profiling (Sørensen and Sørensen 1995; Sørensen 1996a). Along the same lines an equipment for continuous transient electromagnetic measurements is being developed (Sørensen and Effersø 1995). For logging purposes the Ellog methods offers a very detailed electrical and gamma log and water sampling (Sørensen 1989, 1994) and a similar hollow auger based equipment is being developed for in situ determination of the hydraulic conductivity (Dam et al. 1996, Effersø and Sørensen 1996). The integrated use of these novel methods have made detailed regional hydrogeophysical investigations economically feasible (Christensen and Sørensen 1994; Sørensen 1996b; Christensen and Sørensen 1996).

2. Modeling of Electromagnetic Responses

Within the last decade 3D electromagnetic modeling has become state of the art. The geophysical community has seen an extremely rapid development in modeling capabilities with different approaches, the most prominent being the integral equation method (IE), the finite difference (FD), and the finite element (FE) techniques. IE codes have mainly been used to model the responses from finite bodies, whereas the FD and FE codes have been developed for general varying subsurface conductivity. All methods require the solution of a large system of linear equations,

and the increase in computing power and efficiency of the routines have been the main contributing factors to the improved modeling capabilities.

The development in EM modeling can be followed from classical papers (Raiche 1974; Weidelt 1975; Hohmann 1975) until the present day. A review of IE methods has been presented by Hohmann (1987) and Raiche (1994). New developments in frequency domain codes have been presented by Mackie and Madden (1993a, 1993b), and Mackie et al. (1994) for the magnetotelluric (MT) problem. Newmann and Alumbaugh (1995) and Alumbaugh et al. (1995) have developed codes for controlled sources running on massively parallel computers. All these codes have applied a coupled first-order difference scheme for Maxwell's equations based on a staggered grid. Lee and Xie (1995) present a second-order FE method for the magnetic field.

Time domain solutions for general inhomogeneous media have been presented by Lee et al. (1990), and Wang and Hohmann (1993). Wang and Tripp (1994) have extended the latter code to include displacement currents to model very early time responses.

Important elements of the improvements obtained have been the application of the conjugate gradient method (CG) to solve the large systems of linear equations, and the use of the perfectly matched layer boundary condition (Berenger 1993) has contributed decisively to the handling of boundary effects and reduction of the number of unknowns by reducing the grid size. Wannamaker (1991) presents improvements in the calculation of the Green's functions associated with 3D EM modeling. Qian and Boerner (1995) have presented interesting studies of the use of higher order basis functions used in IE methods based on the work of Hanneson and West (1984a, 1984b) and Walker and West (1991). Slob and van den Berg (1995) advocate the use of appropriate basis functions to facilitate the transformation from Laplace domain to time domain in their IE time domain code.

Recently, analyses of an "extended" Born approximation have been presented. The term "extended" indicates its extended range of validity as far as frequency and conductivity contrasts are concerned. The extended Born approximation is formulated through an integral equation for the electric and magnetic field, and the approximation is obtained by expressing the scattered field as product between a tensor and the background field (Habashy et al. 1993, Zhdanov 1996). The extended Born approximation is a promising new strategy of approximate forward mapping and it also has the potential of being used in a fast two-step inverse procedure (Torres-Verdín and Habashy 1994, 1995) to yield subsurface conductivity. The price paid for the superior performance is that it is more time-consuming and requires more involved programming than the simple Born approximation.

A large number of codes in the geophysical community, each one with its strong points and weaknesses, have been reviewed by Smith and Paine (1995). The development of these codes have served extremely important purposes. It has brought new insights into the dynamics of EM fields in the earth and they will serve as reference programs and bench marks for subsequent development of approximate

but much faster codes. For practical purposes – and certainly when inversion of EM data is considered – the coming years will see many ingenious approximations and shortcuts to reduce computation times considerably while maintaining the main features of the correct solutions. The poor resolution capabilities of EM methods makes it unnecessary for practical purposes to model details of EM responses, which cannot be measured, or to include model characteristics which cannot be resolved.

3. Inversion of Geophysical Data

For some reason all physical laws stated in the wonderful shorthand language of mathematics are formulated "forwards", i.e. if we know the distribution of physical parameters in space and time, the solution of the equations governing the phenomenon will allow us to predict the result of a particular measurement.

This state of affairs seems well suited for omniscient beings, whose job it is to unfold the universe. However, when we as humans want to increase our knowledge of the subsurface, we want to find the distribution of the subsurface conductivity from a set of measurements of electromagnetic fields from natural or artificial sources. We have the opposite of the forward problem: an "inverse" problem. As all our mathematical and numerical techniques are forward-formulated, there is no direct solution to the inverse problem, and the only way to proceed is to solve the forward problem for a number of distributions and then compare the predicted data with the actual measurements to see which distribution most faithfully reproduces the measured data. Basically, all the intricacies of geophysical inversion are designed to do just that: choosing the sequence of forward calculations as intelligently as possible to minimize the computational burden.

"Geophysical inverse problems are usually non-linear, ill-posed, and often large-scale". This is the opening statement of the paper by Oldenburg and Ellis on Approximate Inverse Mapping inversion (1991) and summarizes precisely the difficulties of geophysical inversion. However, the paper does present some very encouraging ideas about geophysical inversion.

By nature electromagnetic problems are non-linear and a popular way to attack the inversion problem has been to linearize the problem and solve the inverse problem iteratively. Only in the case of the low frequency approximation to inductive measurements is the apparent conductivity a linear function of the subsurface conductivity.

The source of the ill-posedness lies in the limited resolution capabilities of electromagnetic measurements, the fact that geophysical data are spatially and temporally aliased and corrupted by noise, and in inconsistencies between data and the assumed simplified earth model. This means that a vast set of models will equally well fit the measured data within the data uncertainty. Consequently some

sort of regularization has to be involved in the solution of the inverse problem to prevent extreme and geologically unrealistic models to be produced.

The large-scale nature of modern EM inversion problems arises because finely discretized 2D and 3D models are now introduced to account for expected geological complexities.

The numerical problems involved in solving a linearized inverse problem fall in three categories: The calculation of the model response (the forward problem), the calculation of the sensitivities, and the solution of a large scale minimization problem expressed as a system of linear equations.

For 1D models the inversion problem is small-scale and involves rarely more than 50 parameters. The 1D forward problem has been solved for some time and an overview can be found in Ward and Hohmann (1987) and Boerner and West (1989). Modeling and inversion of 1D problems is very fast, partly because very efficient algorithms have been developed for the calculation of the Hankel transforms appearing in most of the field expressions (Johansen and Sørensen 1979; Anderson 1979, 1989; Christensen 1990; Sørensen and Christensen 1994). An overview of the magnetotelluric 1D inversion problem is given in Whittall and Oldenburg (1990) and a more general overview of electromagnetic inverse techniques can be found in Hohmann and Raiche (1987).

For 2D and 3D models the number of model parameters increases drastically. 2D and especially 3D forward solutions are considerably more time consuming than 1D calculations and the large number of model parameters often makes it prohibitively slow to calculate the true sensitivities. 2D and 3D models with many model parameters produce large scale inversion problems which must be attacked in a different manner for practical purposes, and a plethora of novel methods and approaches to this problem has appeared in the geophysical literature. Excellent overview papers have been presented in the last decades by Oldenburg (1990, 1994).

The inverse procedures suggested in the literature fall in two main categories. One formulates the inverse problem as a minimization problem of an object function penalizing misfit between the model and some reference model, and/or some model properties like smallness, flatness, smoothness, etc., subject to fitting the measured data to some prescribed misfit (Oldenburg 1994). The other formulation follows a statistical approach (Tarantola 1987), which expresses the iterative solution as

$$\Delta\mathbf{x} = [\mathbf{A}^T C_e \mathbf{A} + \mathbf{C}_m^{-1}]^{-1} \mathbf{A}^T \mathbf{C}_e^{-1} \Delta\mathbf{y} \tag{1}$$

where $\Delta\mathbf{y}$ is the difference between the measured data and the last model response, $\Delta\mathbf{x}$ is the change in model parameters, $\mathbf{A}$ is the matrix containing the sensitivities, $\mathbf{C}_e$ is the data error covariance matrix, and $\mathbf{C}_m$ is the model covariance matrix. Both of these formulations lead essentially to the same solutions, and the adherence to one or the other is mostly a matter of taste and tradition (and belief?). I the following sections the latter shall be pursued.

One of the important realizations coming from analyses of the inverse problem is that any approach to inversion carries with it the prejudice of the interpreter. In the above formulation it becomes clear that the opinion of the interpreter enters in the specification of the data error and model covariance matrices. This highlights the aforementioned importance of having quantitative measures of data errors. However, instead of regarding the specification of model constraints as a necessary inconvenience full of traps and pitfalls, interpreters should recognize it as a chance of incorporating relevant geological a priori information about the model. In almost any inversion situation something is known on beforehand about the geology being probed, and this information should be quantitatively expressed in the model constraints. Jacobsen (1993) presents methods of pragmatic covariance specification as a stacking of stationary processes, and Ellis and Oldenburg (1994) present an approach with spatially varying model constraints. Unawareness of the above will often lead to misconceptions and erroneous inversion results.

If model responses and exact or approximate sensitivities can be calculated within reasonable time, the major problem is the minimization problem. One of the promising approaches to large scale problems is the subspace method (Oldenburg et al. 1993; Oldenburg and Li 1994) and the conjugate gradient methods. Recently attention has been drawn to the fact that it is possible to incorporate model constraints in the conjugate gradient solution to large linear systems (Hansen 1992, Hanke and Hansen 1993, Haber and Oldenburg 1996). These results seem very encouraging for the solution of large-scale problems.

3.1. Approximate inverse mappings

As mentioned in the introduction, approximate inverse mappings (AIM) are of great interest in themselves for a number of reasons. However, the full potential of AIMs is realized in connection with accurate forward mappings to form what has been termed AIM inverse procedures (Oldenburg and Ellis 1991, Li and Oldenburg 1994). In the AIM inverse technique, which is based upon the availability of an (adequately) exact forward model response defined by the mapping F, and an AIM, $\tilde{F}^{-1}$, the calculation of sensitivities is completely avoided.

Assuming that we have access to an accurate forward mapping – or one that is sufficiently accurate for the purpose – the important factor in an AIM procedure is the approximate inverse mapping. We would like the approximate inverse mapping to possess certain characteristics: 1) it is as accurate as possible, 2) it is simple and fast, 3) it must be robust, and 4) we can in some way control the smoothness of the models it produces. Evidently there is often a trade-off between 1) and 2). The robustness of the AIM algorithm means that we would prefer it to be of the same quality for all models rather than being very good for certain models but very poor for others. The best way to ensure this is to make it in accordance with the basic physics of the problem.

In the case where the forward problem can be approximated with a linear mapping, $\tilde{F}$, the approximate inverse can be defined by the solution to a linear inverse problem. This means that all the usual regularization methods involved in linear inverse problems can be brought into play, and it will be possible to construct an inverse which produces models with the desired qualities explicitly expressed as model constraints.

A very interesting class of linear approximate forward mappings which will define attractive inverse mappings to be used in an AIM scheme can be constructed using the Born approximation. By linearizing the exact forward mapping about a model m^0, we obtain the expansion

$$F(m) = F(m^0) + \int g(m^0; \mathbf{r})[m(\mathbf{r}) - m^0(\mathbf{r})]d^3\mathbf{r} + \cdots \tag{2}$$

where g is the Fréchet kernel and the ellipsis indicates terms of higher order. Neglecting these, we obtain the approximate forward mapping based on the Born approximation

$$\tilde{F}(m) - F(m^0) = \int g(m^0; \mathbf{r})[m(\mathbf{r}) - m^0(\mathbf{r})]d^3\mathbf{r}. \tag{3}$$

Often the reference model is chosen to be a homogeneous halfspace. For the homogeneous halfspace it is often possible to find analytic (or rapidly calculated) expressions for the Fréchet kernel, and the use of the homogeneous halfspace is equivalent to a minimum structure assumption with regard to the model, which is often a reasonable choice.

The Born approximation works surprisingly well in many circumstances, e.g. DC resistivity problems, where it reproduces the main structural features of the subsurface conductivity (Loke and Barker 1995) but with a limited dynamic range in conductivity. For translational invariant problems (profile oriented data or data on a regular 2D surface grid) the AIM of the Born approximation can be solved in the wavenumber domain. This decouples the 2D (3D) problems into 1D problems, one for each wavenumber (pair), and the solution is found by inverse Fourier transformations of the 1D solutions. This approach is extremely fast and efficient (Li and Oldenburg 1994; Møller et al. 1996; Jacobsen 1996).

The ease of use and the good results obtained in many instances with the Born approximation has inspired several researchers to develop a variant of the Born approximation for which the term "Adaptive Born approximation" seems appropriate. It is as simple and fast to implement as the ordinary Born approximation and gives superior results in inductive EM problems.

4. The Adaptive Born Approximation

In the traditional formulation of the inverse problem using the Born approximation, the homogeneous halfspace is often chosen as the background model, and consequently the conductivity of the halfspace must be chosen. Data are then given as the

difference between the measured data and the models response of the halfspace for the chosen conductivity, and the model to be found in the inversion is the difference between the model conductivity and the halfspace conductivity (see Equation (2)). However, for inductive electromagnetic problems this relative formulation can be shown to be equivalent to an absolute formulation, where the Fréchet kernel acts as a weighting function for the subsurface conductivity (Gómez-Treviño 1987a, 1987b). The absolute formulation removes the influence of the choice of background conductivity from the data and the model, but it does not alter the fact that the Fréchet kernel depends on the halfspace conductivity and that it must be calculated assuming a specific halfspace conductivity.

In the following a new type of approximate inverse mapping shall be presented, where the Fréchet kernel of the simple Born approximation is scaled according to the data. The central point of the approximation is that the Fréchet kernel is scaled according to an average conductivity determined from a simple transformation of the measurements, and therefore we shall call it an Adaptive Born (AB) approximation. The inverse is as simple and fast as the Born approximation, but is superior in that the models produced are better approximations to the true models. The principles behind the adaptive Born approximation can be used in both frequency and time domain electromagnetic methods. However, for galvanic type electrical methods it is identical to the simple Born approximation, as the Fréchet kernel of galvanic methods does not depend on the conductivity.

A number of formulations of the 1D induction problem have led to approximations which are adaptive. The traditional Niblett-Bostick transformation of magnetotelluric data, which has found widespread use, is an example of an imaging algorithm with adaptive character. In Gómez-Treviño (1987a) and Gómez-Treviño et al. (1994) an integral equation is developed for the 1D magnetotelluric problem, and it is shown how the Niblett-Bostick transformation can be derived from the integral equation formulation through an adaptive approximation, an approach developed further in Esparza and Gómez-Treviño (1996).

In the present paper an adaptive Born approximation shall be used in the construction of an AIM of 1D and 2D transient electromagnetic data. However, the principles are valid for frequency domain problems as well, and in most cases a formulation for the frequency domain can be found by substituting “frequency” instead of “time” and “skin depth” instead of “diffusion depth”. The development here relies on arguments based on the physics of diffusion of electromagnetic fields into the ground.

In the process of diffusion of transient electromagnetic fields into the ground, the diffusion depth depends on the subsurface conductivity structure. For any time of measurement this diffusion depth depends on the conductivity distribution from the surface down to approximately the diffusion depth. A number of imaging methods have been suggested, which are based on the variation of the diffusion velocity with conductivity (Nekut 1987; Macnae and Lamontagne 1987; Eaton and Hohmann 1989; Macnae et al. 1991). These methods are based on finding the

depth to an equivalent current filament – an "image" of the source – as a function of time, from which the diffusion velocity and thereby the conductivity can be found. The conductivity is then ascribed to a depth equal to the (scaled) image depth. In Macnae and Lamontagne (1987) a number of such images are used instead of just one. For the coincident loop configuration the paper by Smith et al. (1994) presents an imaging method where the depth to the peak of the sensitivity function is used as an equivalent depth.

Polzer (1985) presents a very interesting approach to the transient 1D inverse problem. Instead of regarding the step response magnetic field as a function of time, Polzer regards time as a function of the magnetic field amplitude. The so defined arrival time (or delay time relative to a reference model) is shown to be much more configuration independent and a much more linear function of subsurface conductivity than the step response. This formulation of Polzer is completely equivalent to the 1D AB algorithm developed in the following as shown in Christensen (1995).

In the AB approximation one of the weaknesses of the simple Born approximation is recognized and circumvented. By assuming a constant conductivity of the halfspace the slower diffusion through good conductors and the faster diffusion through poor conductors is not taken into account. However, if we could find a measure of the average conductivity for the subsurface volume involved in the response at a given time, we could choose this conductivity as an "instantaneous" conductivity of the halfspace for the calculation of the Fréchet kernel, whereby the Fréchet kernel would more accurately reflect the physical diffusion process. In Christensen (1995) it is shown that the all-time apparent conductivity based on the transient step response is a good candidate for such an average measure. This is intuitively clear, as the all-time apparent conductivity is defined as the conductivity of the homogeneous halfspace which would produce the measured response at the given time.

Not all definitions of apparent conductivity are suited for the purpose of scaling the Fréchet derivative (for a thorough discussion of apparent resistivity in TEM measurements see Spies and Eggers 1986). Figure 1 shows apparent resistivity curves for a descending two-layer earth model using the late-time and the early-time definitions based on the impulse response and the all-time definition of the step response. The much-used late-time apparent resistivity of impulse response measurements exhibits over- and undershoot which are not desirable and the descending branch for early times does not reflect the near-surface resistivity. The early-time apparent resistivity based on the impulse response reflects the true resistivity only at times so early that it is of little use in most cases. The all-time apparent resistivity based on the step response, however, has a desirable behavior with a smooth transition between the true resistivities, and it coincides with the true resistivities at early and late times.

Most TEM equipments measure the time rate of change of a magnetic field component with an induction coil after an abrupt turn-off of the transmitter current, i.e. the convolution between the impulse response and the particular transmitter

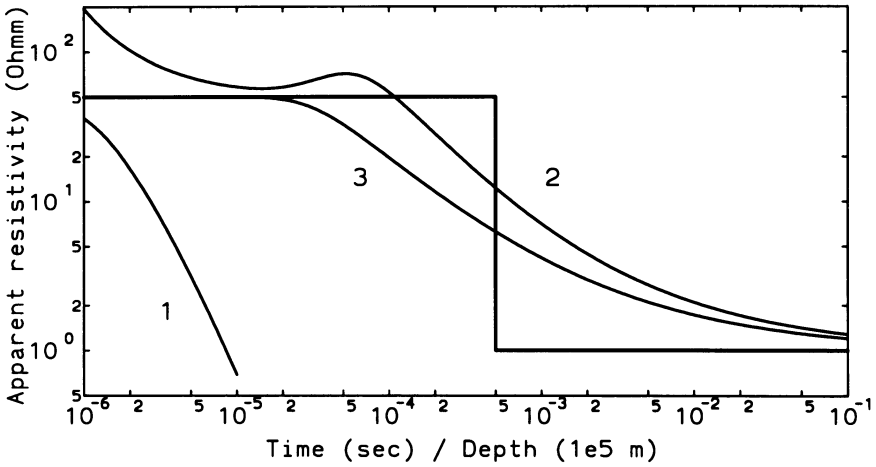

Figure 1. Apparent resistivity transforms for a 2-layer descending model with resistivity 100 m in the first layer, 10 m in the second layer, and 50 m layer thickness. The true model is shown with the thick curve. Curve (1) is the impulse response early-time apparent resistivity, curve (2) is the impulse response late-time apparent resistivity, and curve (3) is the step response all-time apparent resistivity.

waveform used. It is thus necessary to calculate the step response from the measured convolved impulse response. Then, from the step response the all-time apparent conductivity must be calculated, which implies that it must be uniquely defined. For the central loop configuration which is widely used for near-surface investigations, where the receiver coil is placed at the center of a circular or square transmitter loop, this is the case. In the case of the coincident loop configuration, where the receiver coil coincides with the transmitter loop, it is possible to uniquely define an all-time apparent conductivity from the impulse response. However, this definition suffers from the same weaknesses as the central loop late-time apparent conductivity, and also for coincident loop measurements it is advantageous to compute the step response. A method for finding the step response from the impulse response is suggested in Eaton and Hohmann (1989) and Levy (1984). In Christensen (1995) the step response is expressed as a linear combination of basis functions, and the coefficients are found by solving a least squares inversion problem with the convolved impulse response as data.

In the following an outline of the 1D AIM algorithm for transient measurements is presented.

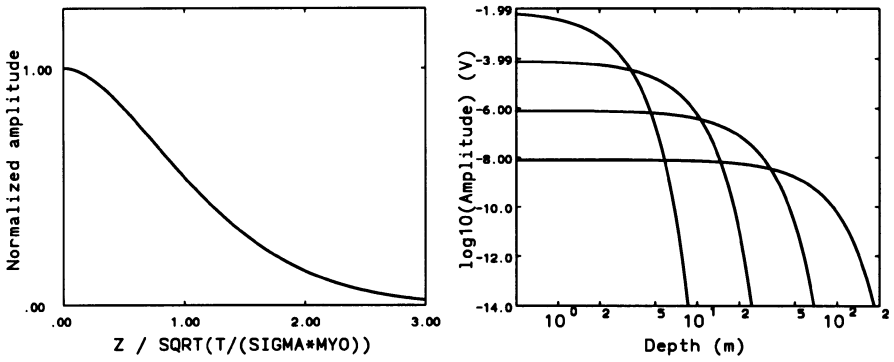

Figure 2. The normalized 1D Fréchet kernel (left) for the transient step response of a vertical magnetic dipole for a homogeneous halfspace as a function of normalized depth. The unnormalized Fréchet kernel (right) is calculated for a halfspace resistivity of 1 Ωm at the times 1 μs, 10 μs, 100 μs, and 1 ms.

4.1. 1D TEM IMAGING BASED ON THE ADAPTIVE BORN APPROXIMATION

In the approximation that conductivity changes are small, the Born approximation describes the change in the response as a linear functional of the change in subsurface conductivity:

$$H_i \approx H_i^{\text{ref}} + \int_0^\infty F(\sigma^{\text{ref}}(z), t_i, z)[\sigma(z) - \sigma^{\text{ref}}(z)]\,\mathrm{d}z \tag{4}$$

where H_i is the measured H-field at the time t_i. H_i^{ref} is the H-field of the reference model. $F(\sigma^{\text{ref}}(z), t_i, z)$ is the Fréchet kernel of the reference model. $\sigma(z)$ is the conductivity of the subsurface. $\sigma^{\text{ref}}(z)$ is the conductivity of the reference model.

McGillivray et al. (1994) have presented a simple general method for calculating 3D Fréchet derivatives of electromagnetic measurements. Fréchet kernels for the 1D case have been developed by Chave (1984). For the homogeneous halfspace Christensen (1995, 1996) finds an analytic expression for the 1D Fréchet kernel for the vertical magnetic field from a coincident vertical magnetic dipole source.

$$F(\sigma, t, z) = \frac{M}{4\pi\sigma}\theta^4 \left\{ \frac{2u}{\sqrt{\pi}}(2u^2 + 1)e^{-u^2} - (4u^4 + 4u^2 - 1)\mathrm{erfc}(u) \right\}, \tag{5}$$

$$\theta = \sqrt{\frac{\mu\sigma}{4t}}, \quad u = \theta z.$$

Figure 2 shows a plot of $F(\sigma, t, z)$ on a linear and a logarithmic scale, the latter at four different times for a source dipole of unit moment. It is seen that the sensitivity is a bell-shaped function of z, which has its maximum at the surface at all times. Figure 2b shows how the amplitude decreases and the depth of diffusion

increases as a function of time. The sensitivity drops very abruptly to zero with depth, decreasing as $u^{-3}\exp(-u^2)$ (Christensen 1995).

In the case considered here the response of the homogeneous halfspace with conductivity σ^0 can be found as the integral of the Fréchet kernel (5) multiplied with the conductivity σ^0

$$\int_0^\infty F(\sigma^0, t_i, z)\sigma^0 \,\mathrm{d}z = \frac{M}{30}\left(\frac{\sigma^0\mu}{\pi t}\right)^{3/2} = H_i^0, \tag{6}$$

so in the case, where the reference model is a homogeneous halfspace, we find

$$H_i \approx H_i^0 + \int_0^\infty F(\sigma^0, t_i, z)[\sigma(z) - \sigma^0]\,\mathrm{d}z = \int_0^\infty F(\sigma^0, t_i, z)\sigma(z)\,\mathrm{d}z. \tag{7}$$

For a measured $H_i(t_i)$ over any 1D structure the solution of Equation (6) in terms of σ^0 determines the all-time apparent conductivity $\sigma^a(t_i)$.

When the subsurface is discretized into a layered 1D structure with L layers given by the layer boundaries z_i, $i = 1, \ldots, l+1$, $z_L = 0$, $z_{L+1} = \infty$, and the conductivity is assumed constant within each layer, Equation (7) becomes

$$H_i \approx \sum_{j=1}^{L} \sigma_j \int_{z_j}^{z_{j+1}} F(\sigma^0, t_i, z)\,\mathrm{d}z. \tag{8}$$

The Adaptive Born approximation is obtained by substituting the apparent conductivity $\sigma^a(t_i)$ instead of the constant halfspace conductivity σ^0 in the expression for the Fréchet kernel in Equation (5). Substituting Equations (5) and (6) in (8) we arrive at:

$$\begin{aligned} H_i &\approx \sum_{j=1}^{L} \sigma_j \int_{z_j}^{z_{j+1}} F(\sigma^a(t_i), t_i, z)\,\mathrm{d}z \\ &= \sum_{j=1}^{L} \sigma_j \frac{H_i}{\sigma^a(t_i)} \int_{z_j}^{z_{j+1}} \hat{F}(\sigma^a(t_i), t_i, z)\,\mathrm{d}z \\ &\Rightarrow \sigma^a(t_i) \approx \sum_{j=1}^{L} \sigma_j \int_{z_j}^{z_{j+1}} \hat{F}(\sigma^a(t_i), t_i, z)\,\mathrm{d}z \end{aligned} \tag{9}$$

Equation (9) defines an approximate forward mapping, where the all-time apparent conductivity is expressed as a weighted sum of the conductivities of each layer with easily calculated weights. These weights, however, depend on the data through the all-time apparent resistivity. The layer conductivities σ_j can be found by solving the linear system of Equations (9).

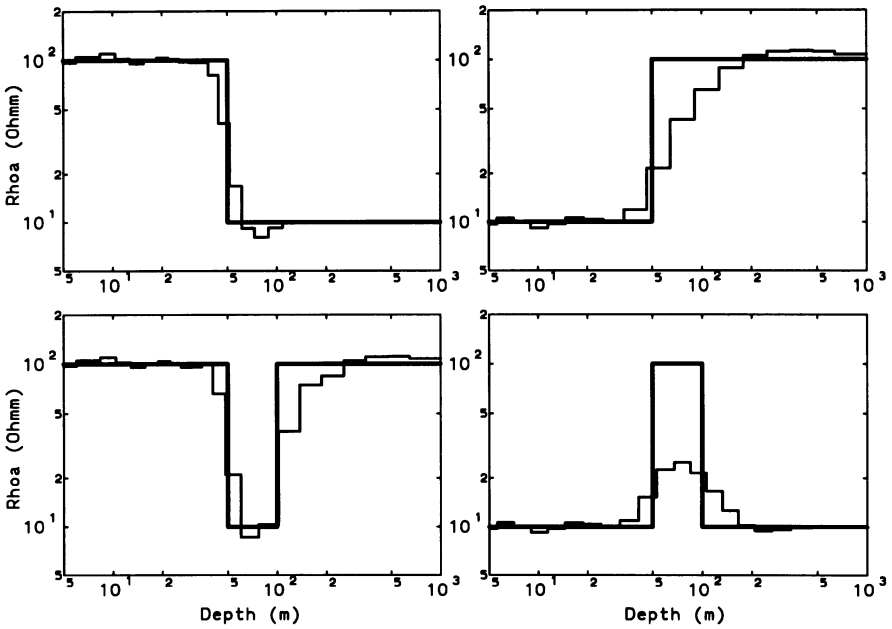

Figure 3. The models obtained using the imaging algorithm on 40 × 40 m^2 central loop soundings over a two-layer decreasing, two-layer increasing, three-layer minimum, and three-layer maximum model. The figure shows the imaged models together with the true models (thicker curves).

It is worth noting that while the inverse is a one-pass mapping, the forward mapping can only be realized iteratively, as the apparent conductivities are not known before the forward response is calculated. A forward mapping procedure can be initialized by scaling the Fréchet kernel with a constant all-time apparent conductivity corresponding to a homogeneous halfspace. The calculated all-time apparent conductivity can then be used to rescale the Fréchet kernel to obtain a better forward mapping, and so on, until convergence is achieved, usually after 5–10 iterations.

As seen in Equation (9) the all-time apparent conductivity does not only serve the scaling purpose, but is also used as input data. This parameter is to a much larger extent independent on measuring configuration than the step response (Christensen 1995), and so the AIM developed for the vertical magnetic dipole is also applicable for other configurations, e.g. central loop and coincident loop. The configuration dependence lies in the transformation from step response to all-time apparent conductivity.

Figure 3 shows the models resulting from the application of the imaging algorithm on synthetic noise-free all-time apparent conductivity data from four different models together with the true resistivity models: two 2-layer models (descending and ascending) and two 3-layer models (minimum and maximum). The results for the double descending and double descending 3-layer models are similar to the 2-

layer models. As step response data transformed to all-time apparent conductivity have been used, the results are not influenced by the transformation from impulse to step response. It is seen that the imaging algorithm reproduces descending type models very well, but reacts slower to ascending resistivity models. The worst performance is seen with the maximum model, which is to be expected. It is seen that the imaged models reach the true asymptotic value of the resistivity very well.

The imaging has been realized using the statistical approach given in Equation (9) and the inverse has been regularized using standard techniques: a diagonal data error covariance matrix has been used corresponding to an assumption of uncoupled noise and a model covariance matrix is defined through a smoothness constraint on the model.

The models produced by the imaging procedure fit the original data very well. In Figure 4 the all-time apparent resistivity data and the all-time apparent resistivity model response of the imaged models using an exact forward modeling routine are shown for the four models of Figure 3. The average misfit per data point is 5%, 1.3%, 2%, and 4.3% for the four models, respectively. This is very satisfactory for a one-pass algorithm working almost instantaneously.

In Figure 5 and 6 model sections obtained by concatenating 1D interpretations of TEM soundings on a profile line using the imaging algorithm and a rigorous inversion with multiple-layer models with fixed layer boundaries and an L_1 norm minimization are compared. The L_1 norm (Oldenburg and Ellis 1993, Madsen and Nielsen 1993) has been used to produce more "blocky" models as the conductivity changes are expected to be abrupt.

In Figure 5 a profile from the island of Rømø, Denmark, consisting of 18 TEM soundings in the central loop configuration is shown. The profile transects the NE corner of the island. The good conductor – the salt water horizon – is closer to the surface at the ends of the profile, where the distance to the coast is small and lies deeper in the middle of the profile, which is situated further inland. Note how the imaged profile section also reflects the surface-near patches of good conductors (dark gray) seen along the profile at coordinates 1750 m, 2700 m, and 4200 m. These have been interpreted as wet areas like marshes and moors.

Another example is shown in Figure 6. The profile of 18 central loop TEM soundings crosses a small river valley at a location where the stream has a natural linear course for several kilometers, which has caused some speculation. The explanation most often given is that the linear course is tectonically determined. This is confirmed by the TEM profile which reveals a very narrow almost graben-like depression in the heavy well-conducting Tertiary clays underlying the otherwise Quaternary formations of the valley. The depression is clearly seen on both profiles and also the distribution of sands and gravels with higher resistivity and clays with lower resistivity within the Quaternary deposits are very similar on the two model sections.

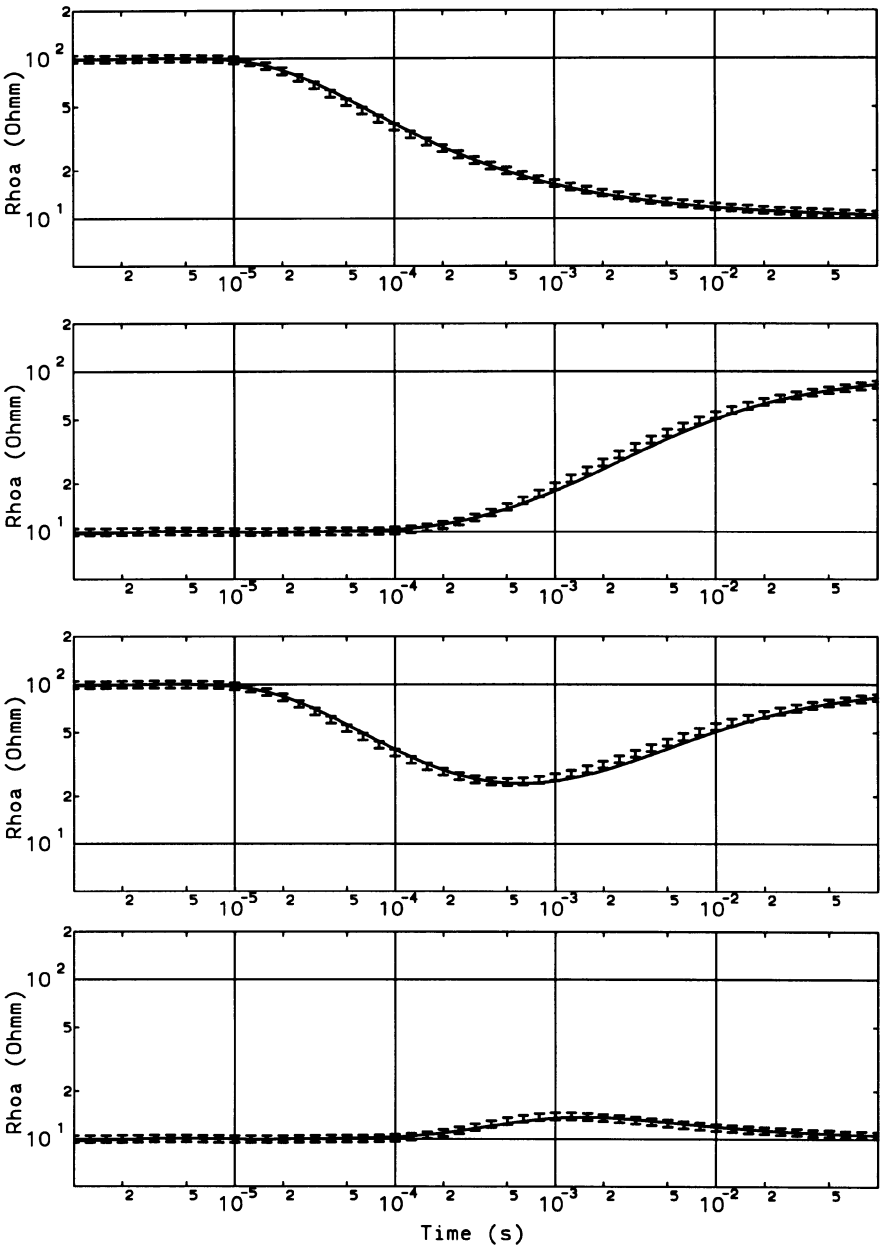

Figure 4. Comparison between the all-time apparent resistivity data used in Figure 3 and the exact forward responses of the imaged models for the four models of Figure 3. The average misfits per data point for the four models are (from above) 2%, 4.3%, 5%, and 1.3%, respectively.

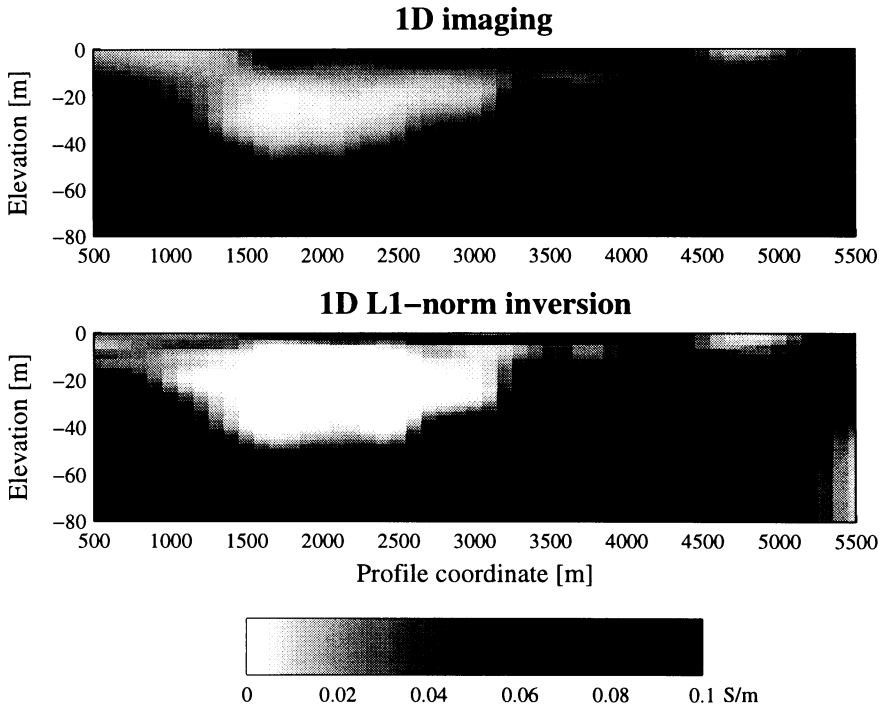

Figure 5. Comparison of 1D imaging (top) and iterative 1D L_1-norm inversions (bottom) of a TEM profile for the detection of the salt water horizon on the island of Rømø, Denmark.

4.2. 2D IMAGING OF TEM MEASUREMENTS

The principle of an adaptive Born approximation can be extended from the 1D case to the 2D case. For magnetotelluric data this has been demonstrated by Gómez-Treviño et al. (1994) and Esparza et al. (1993, 1996). In the following an algorithm for the 2D TEM case shall be demonstrated.

If TEM data have been collected on a profile line a model section can be obtained by concatenating a series of 1D interpretations of the measurements as seen in Figure 5 and 6. Besides being a good way of visualizing the results of the 1D interpretations, it is also a perfectly justified way of interpretation when lateral changes are small or measurements are sparse. However, when abrupt lateral changes are present and the density of measurements is appropriate a 2D inversion is desirable. In the 2D case an AIM would be of even greater help than in the 1D case, as there are several commercially available least squares iterative inversion programs for 1D interpretation, but hardly any such for the 2D case. In the following I shall present preliminary results from the application of an AB approximation to formulate a 2D AIM for TEM measurements.

As in the case of the 1D problem we shall use the 3D Fréchet kernel of the homogeneous half-space for the vertical magnetic dipole in the derivation of the

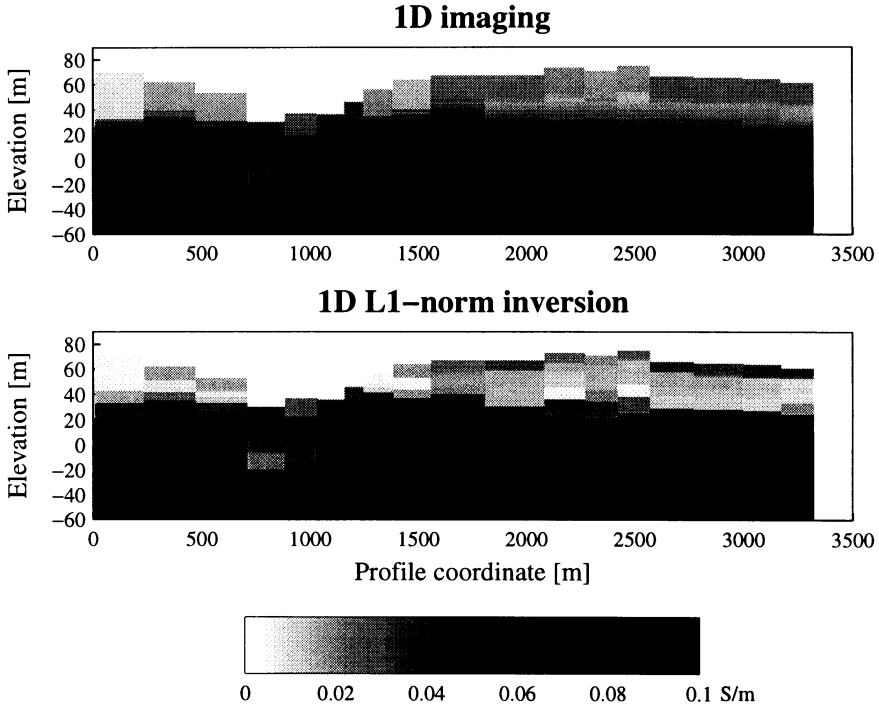

Figure 6. Comparison of 1D iterative inversions and imaging of a TEM profile across the Gjern river valley, Jutland Denmark.

AIM. However, the use of apparent conductivity as data in the final formulation removes the dependence on configuration to a large extent. The Fréchet kernel is integrated over one horizontal coordinate to give the 2D kernel. The subsurface is discretized into rectangular infinite cylinders by first defining a 1D layered model with exponentially increasing depth to layer boundaries, which is then discretized horizontally into model elements with constant width. For each measuring site and time of measurement the diffusion depth – and accordingly the diffusion width – of the Fréchet kernel is scaled according to the all-time apparent conductivity of the step response. The inverse problem is solved in a least squares sense according to

$$\boldsymbol{\sigma} = (\mathbf{A}^T \mathbf{C}_e^{-1} \mathbf{A} + \mathbf{C}_m^{-1})^{-1} \mathbf{A}^T \mathbf{C}_e^{-1} \boldsymbol{\sigma}^a \tag{10}$$

where $\mathbf{A}$ is the matrix of Fréchet weights, $\mathbf{C}_e$ is the data error covariance matrix, $\mathbf{C}_m$ is the model covariance matrix, and $\boldsymbol{\sigma}^a$ is the all-time apparent conductivity data. The data error covariance matrix is diagonal corresponding to an assumption of Gaussian distributed independent noise on the measurements. The model

covariance matrix is a full matrix correlating all model elements with each other and has the elements

$$C_{ij} = C_0 \exp\left(-\sqrt{\left(\frac{(x_i - x_j)}{L_x}\right)^2 + \left(\frac{(z_i - z_j)}{L_z}\right)^2}\right) \tag{11}$$

where L_x is the correlation length in the x-direction and L_z is the correlation length in the z-direction. C_0 is the amplitude of the covariance.

The fact that the diffusion depth of the Fréchet kernel is scaled according to the all-time apparent conductivity for every measuring site and time of measurement means that the problem is no longer translational invariant, as would have been the case, if a constant halfspace conductivity had been assumed. We are thus restricted to solving the problem in the space domain and cannot use the method of transforming to the wavenumber domain, which has proved its efficiency in a number of other 2D and 3D problems (Li and Oldenburg 1994; Møller et al. 1996, Jacobsen 1996).

In Figures 7–10 the results of applying the 2D inverse algorithm are presented together with concatenated 1D interpretations over four models. In all models there is a 20 m thick top layer with resistivity 30 m. In Figure 7 a conductive block in a resistive halfspace is placed under the top layer, and in Figure 8 the block is resistive in a conducting halfspace. The calculation of model step responses has been done with the EMIE code (Wannamaker 1991).

The 1D interpretations have been done with a L_1 norm to produce as blocky models as possible (Christensen and Auken 1992; Oldenburg and Ellis 1993). The subsurface has been discretized into 11 layers with fixed layer boundaries with exponentially increasing depths (2 per octave), and a smoothness constraint has been imposed using the first derivative of the resistivity structure.

The 1D model sections seen in Figures 7 and 8 display the typical “pants legs” structure also found in the galvanic case of 1D interpretation of 2D geoelectrical data. This is caused by the fact that the sensitivity of the measurements spreads sidewards while diffusing downwards. Whenever the sensitivity function reaches a good conductor the 1D interpretation will place the good conductor at a depth which increases with the time of the incidence, i.e. the distance to the conductor, thus producing the pants legs.

Laterally the conductivity anomalies are placed in the right positions, but the depth extent of the blocks is strongly underestimated. The conductive anomaly produces stronger pants legs structures than the resistive anomaly as must be expected from transient measurements. Besides being vertically squeezed a conductive anomaly will appear with a very high conductivity with extremely low conductivity underneath. This latter feature can be used as a “marker” for identifying locations, where a 1D interpretation is insufficient.

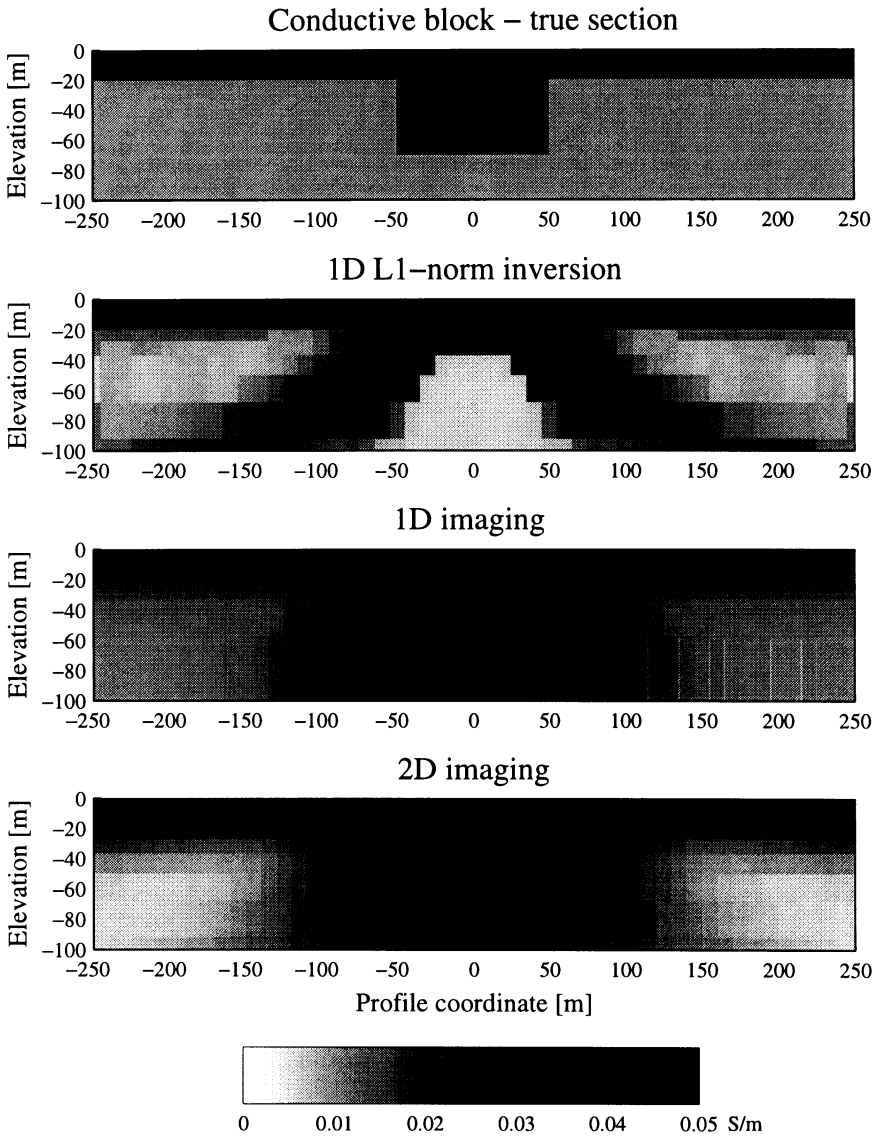

Figure 7. Comparison between model sections obtained through concatenated 1D L_1-norm inversions, 1D, and 2D imaging of transient electromagnetic soundings in the central loop configuration with a 40 × 40 m^2 transmitter loop along a profile. The true model is a conductive block (10 Ωm) 100 m wide and 50 m thick in a resistive halfspace (100 Ωm) with 20 m overburden (30 Ωm). The distance between soundings is 10 m.

The theoretical data have also been interpreted using the 1D imaging algorithm outlined in the previous section. Though the 1D imaging naturally also displays the pants legs effect it seems to be less pronounced than for 1D interpretations.

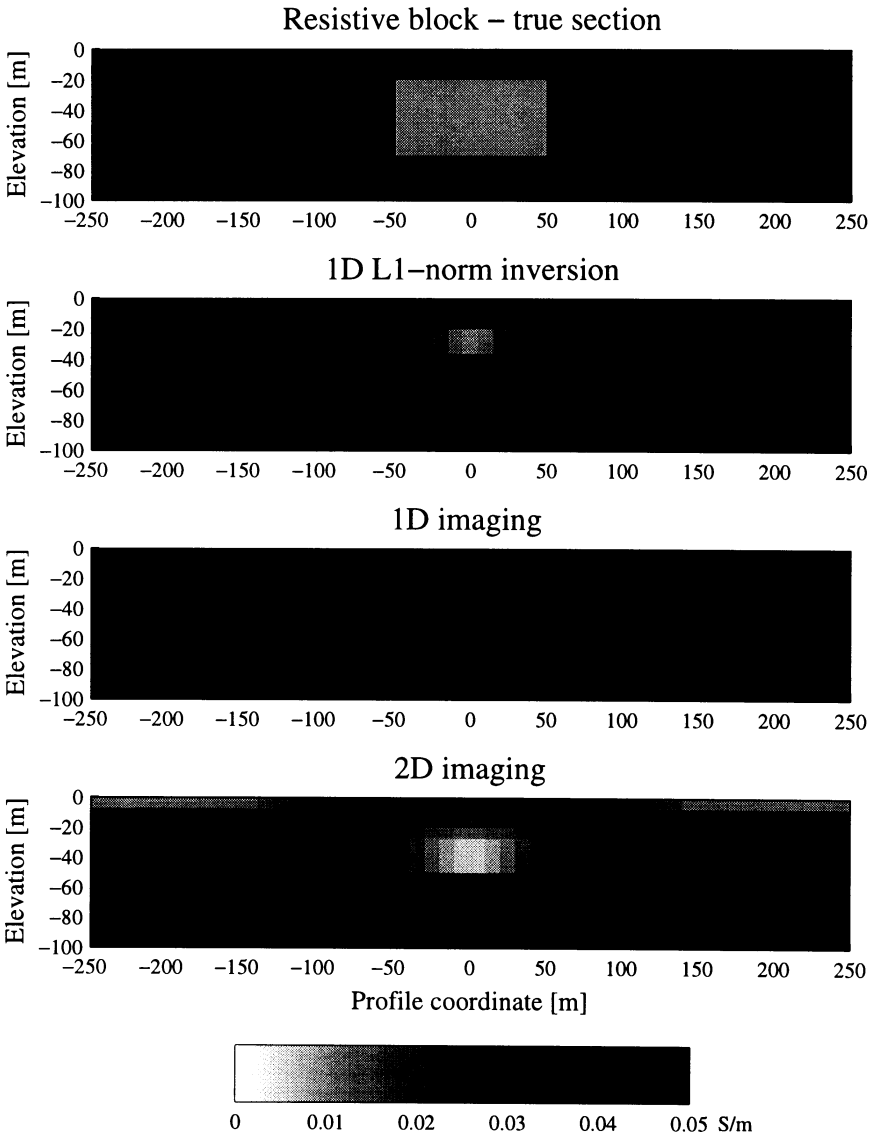

Figure 8. Comparison between model sections obtained through concatenated 1D L_1-norm inversions, 1D, and 2D imaging of transient electromagnetic soundings in the central loop configuration with a 40 × 40m^2 transmitter loop along a profile. The true model is a resistive block (100 Ωm) 100 m wide and 50 m thick in a conductive halfspace (10 Ωm) with 20 m overburden (30 Ωm). The distance between soundings is 10 m.

Let us turn to the results of the 2D adaptive Born AIM seen in Figures 7 and 8. The depth to the top and the lateral position of the conductivity anomalies are well recovered, and it is seen that the pants legs effects are practically removed. Both in

the case of the conductive and resistive block it is seen that the depth extent is much better recovered than is the case for 1D inversions. The true conductivities are not quite reached, but this must be expected from a Born approximation inverse. The overall picture is that the 2D AIM is clearly superior to a profile of collated 1D interpretations or 1D imagings.

The results presented in Figures 7 and 8 have been obtained with noise-free step response data. An interesting question is how robust the developed algorithm is to data noise. This question is addressed in Figure 9, where the results for the conductive block model based on noise-free data is compared with those obtained after Gaussian distributed zero-mean noise with a standard deviation of 5 mS and 10 mS, respectively, have been added. The 5 mS noise is 50% of the halfspace conductivity and 5% of the conductivity of the block, while 10 mS corresponds to a noise level of 100% of the halfspace conductivity and 10% of the target conductivity. As expected the results are somewhat more smeared out, but the overall structure of the model is retained thus showing the robustness of the AIM.

Another interesting question is the superiority of the Adaptive Born approximation over the ordinary Born approximation. As mentioned, the scaling of the Fréchet kernel destroys its translational invariance and thus obstructs the possibility of an extremely fast wavenumber domain solution. If the Adaptive Born approximation is not superior to the ordinary Born approximation this is a high price to pay. In Figure 10 the result obtained for the conductive block model with the Adaptive Born approximation is compared with results obtained with the ordinary Born approximation for different choices of background halfspace conductivity. The results indicate that if the background conductivity is chosen equal to the surface conductivity the Born approximation performs similar to the Adaptive Born approximation – at least for the present model – where surface conductivity is very homogeneous and the top layer thickness is not small. If the background conductivity is wrongly chosen, however, the result is definitely inferior to that of the Adaptive Born approximation. It is not always possible to choose the background conductivity equal to the surface conductivity as a highly inhomogeneous surface conductivity will make it difficult to choose the background conductivity of the Born approximation, which must be chosen constant for the whole profile.

Two examples of the application of the 2D AIM to real TEM data shall be given.

In Figure 11 the 2D imaging procedure has been applied to a profile of transient electromagnetic soundings in the central loop configuration recorded with a 40 $\times$ 40 m square transmitter loop over the basement horst Hallandsåsen in Scania, Sweden. The investigation was part of a engineering geophysical survey with the purpose of finding low resistivity zones in the otherwise highly resistive granites and gneisses. These would indicate areas of water bearing fault zones or heavy clays as end products of the alteration of the old bedrock, and both would pose severe difficulties for the drilling of a double railway tunnel through Hallandsåsen. Besides the TEM soundings CVES profiling was carried out and an extensive drilling programme was implemented.

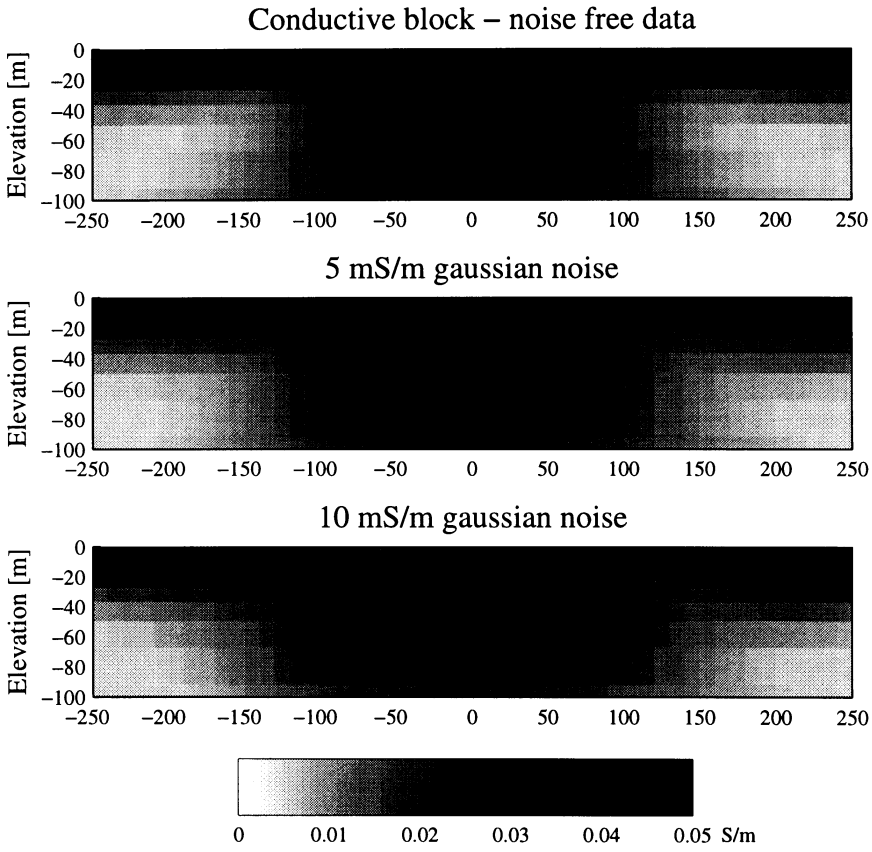

Figure 9. Comparison between model sections obtained through 2D imaging of transient electromagnetic sounding data with different noise levels. The true model is the conductive block seen in Figure 7. The top section is obtained with noise free data. The middle section is obtained after Gaussian distributed uncorrellated noise with 0.005 S/m standard deviation has been added to the data. In the bottom section Gaussian distributed uncorrellated noise with 0.01 S/m standard deviation has been added to the data.

Figure 11a shows the result of a 2D interpretation (Loke and Barker 1996) of the CVES data. High conductivity zones are clearly indicated on the model section. Two drillings on the profile line have confirmed the CVES interpretation. In Figure 11b the result of the 2D imaging algorithm for TEM soundings is shown. The average spacing between TEM soundings was 40 m. The inversion has been carried out using a data error of 5 mS and a model covariance amplitude 16 times smaller than the data variance. The correlation lengths in the x- and z-directions were 80 m and 5 m, respectively. Essentially the same geological structures are found in the TEM model section as in the CVES model section. Figure 11c shows concatenated 1D interpretations using the L_1-norm and a multiple layer model with fixed layer boundaries.

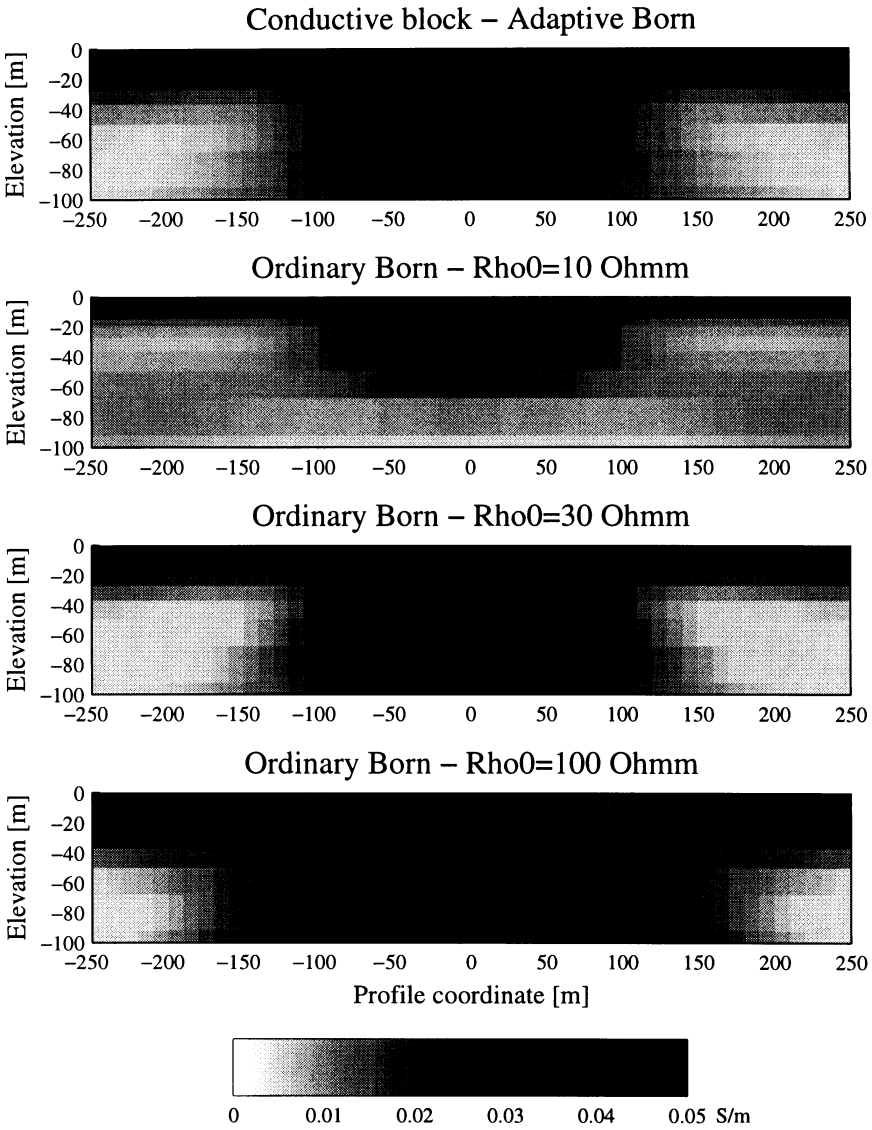

Figure 10. Comparison between model sections obtained by 2D imaging of transient electromagnetic soundings using the Adaptive Born approximation and the traditional Born approximation with different background conductivities. The true model is the conductive block seen in Figure 7. The top section is obtained through the Adaptive Born approximation. The lower three sections have been obtained using the ordinary Born approximation with a reference halfspace conductivity corresponding to 10 Ωm, 30 Ωm, and 100 Ωm, respectively. Noise free data have been used for all sections.

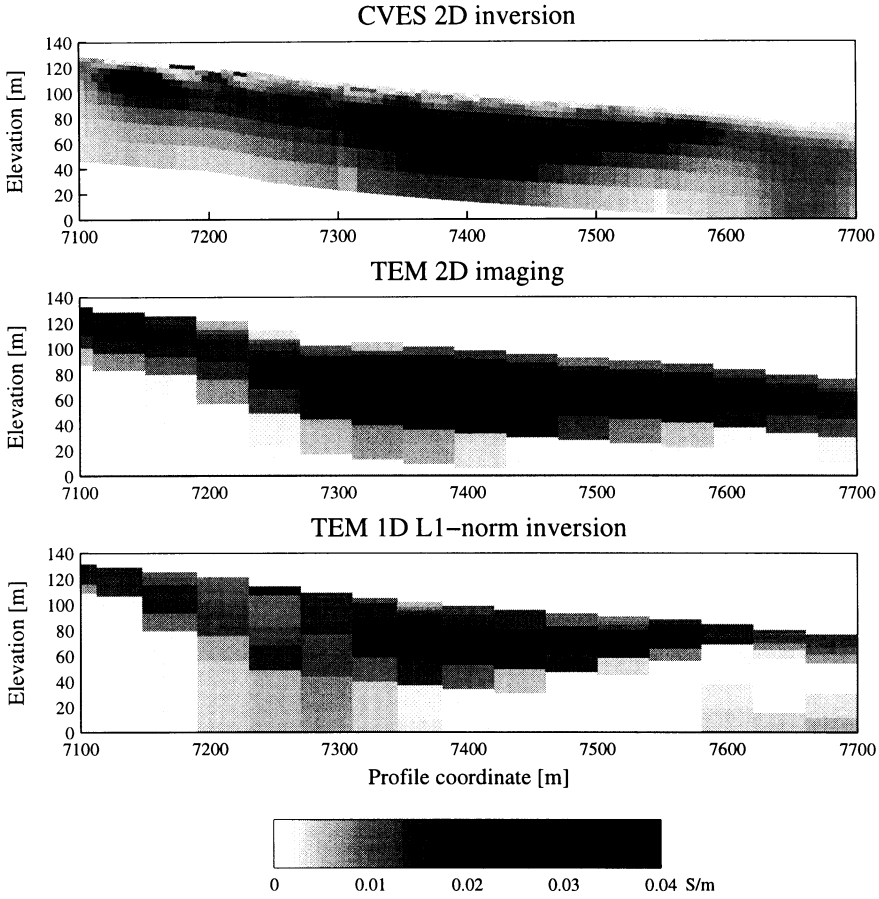

Figure 11. Model sections from Sødra Randzonen, Hallandsåsen. The top section is obtained from 2D inversion of CVES data. Results from the 2D imaging is seen in the middle section. The bottom section shows concatenated 1D L_1-norm interpretations of the TEM data.

The 2D TEM imaging reproduces the lateral and horizontal boundaries of the good conductor found in the area. The conductor has been interpreted as well conducting clays. Notice how the 2D imaging reproduces the surface-near higher resistivities seen in the CVES profile though this is certainly not one of the strong points of TEM data. Also the near-surface well conducting minor feature at the left border of the section is found in both profiles. The 1D L_1-norm inversion result is somewhat more irregular and misses the leftmost conductive feature.

The second example is from a survey of salt water intrusion in a limestone aquifer. The profiles have been measured over raised, post-glacial Litorina sea bottom in the northern parts of Denmark, where limestone, sometimes overlain by sand, is covered with surficial clays. Central loop soundings with a 40×40 m^2 transmitter loop have been made for every 40 m on the profiles. In the top part of

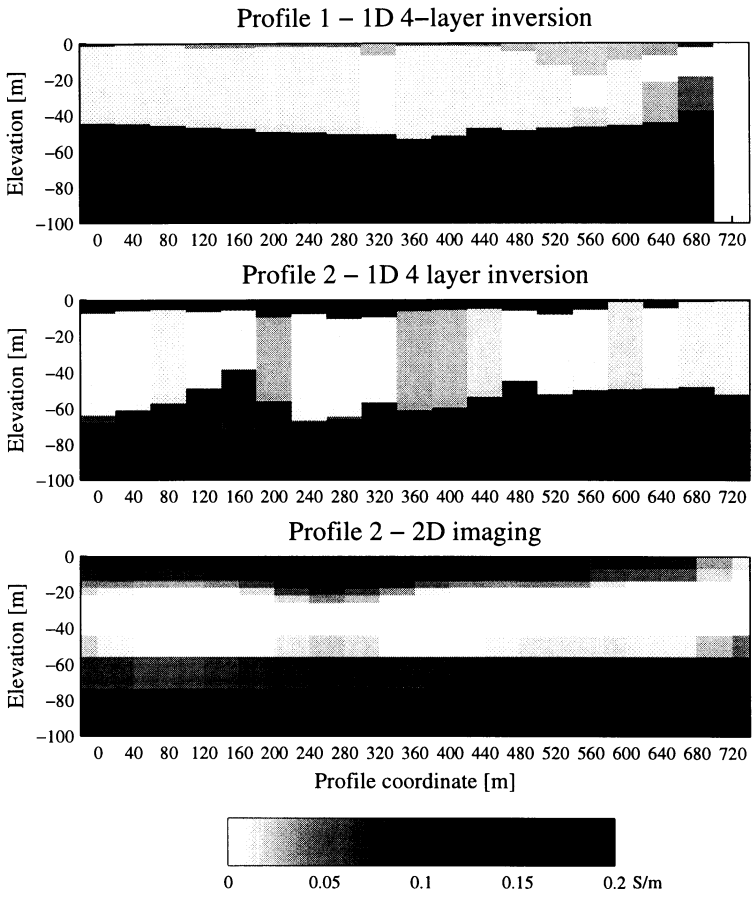

Figure 12. Model sections form Tved, Denmark. The top section is the model section from concatenated 1D four-layer inversions of profile 1. The middle section is model section from concatenated 1D four-layer inversions of profile 2. The bottom section is obtained from 2D imaging.

Figure 12 a model section from concatenated 1D interpretations is shown for the first of the two survey lines. This section is almost entirely 1D and the 2D imaging (not shown here) reproduces this picture. The middle part of Figure 12 shows a concatenated 1D model section for the second survey line. This interpretation leads you to believe that the conductivity of the limestone is much more heterogeneous than on the first profile. The 2D imaging result in The bottom section of Figure 12 shows a different picture altogether. The seemingly randomly distributed well conducting parts of the limestone reveal themselves to be lateral effects, pants legs effect, of a near-surface very good conductor. Comparing the sections it is recognized that the thickness of the well conducting feature is underestimated by the 1D inversions and that the conductivity of the limestone is very low just below the conductive feature, just as illustrated in the theoretical example with the

conductive block. A possible explanation for the well conducting surface feature would identify it as a fault zone in the limestone. Due to increased weathering of the fault zone the elevation has become lower than the surroundings and a thicker layer of clay has been deposited. The slightly increased conductivity below the near-surface feature supports this interpretation as a fault zone would have a thicker transition zone between fresh and salt water in the limestone.

In both of the above examples the computation time was approximately 2 minutes on a 90 MHz Pentium laptop with 16 MB RAM. The programming has been done as a hybrid between a FORTRAN program calculating the matrix of Fréchet weights and the model covariance matrix and a MATLAB program performing the inversion and plotting. Though the above results can only be described as very preliminary they do seem encouraging. There remains much to be done in terms of finding optimal regularization of the inverse problem and faster methods like conjugate gradient to solve the system of linear equations. Also rules of thumb for deciding when 1D imaging and inversion are as good as 2D imaging depending on the density of measurements and the lateral gradient of conductivity would be very useful.

5. Discussion and Conclusion

An important field of research today concerning electromagnetic subsurface imaging is the use of approximate methods in forward model calculations and in inverse mappings. The limited resolution capabilities of electromagnetic methods and the sparsity in space and time of electromagnetic data makes it appropriate to use approximate inverse methods and – as a part of those – approximate forward modeling procedures.

The approximations involved in inversion of electromagnetic data can be on different levels, each to be used at different times of the interpretation process. Modern electromagnetic equipment often collects data densely along profile lines and as an on-line, in-field, real-time processing procedure an extremely fast one-pass 1D imaging algorithm seems well suited. The processing gives estimates of subsurface conductivity beyond the mere data transformation to apparent conductivity and enables an improved quality control and a continuous update of the measuring strategy.

The next step in an integrated interpretation sequence could be the application of a good 2D imaging procedure. A minimum requirement for this sort of algorithm is that it is truly 2D, i.e. it removes the artifacts found in 1D imaging of data from 2D structures caused by the lateral extent of the sensitivity function of the measuring configuration. These algorithms do not necessarily have to be extremely fast, but should on the other hand not involve substantially more time than it took to collect the measurements. Based on the results of this intermediary stage processing interesting anomalies can be identified for subsequent more time-consuming rigorous

inversion involving iterative methods based on exact (or very good approximate) forward algorithms and some sort of updating strategy.

The Adaptive Born approximation is suggested as the starting point of an approximate inverse mapping which can be applied in both frequency and time domain inverse procedures. The 1D imaging of transient data developed here is a very good candidate for the low-level, extremely fast, on-line processing mentioned above. The algorithm is almost instantaneous and the models obtained fit data typically better than 5%, which is as good as one might expect from rigorous inversion routines.

The preliminary results shown here indicate that the AB AIM for transient data can be successfully applied in the 2D case. This is an example of the intermediary stage imaging procedure mentioned above. The 2D imaging produces model sections, where the pants legs effect has been removed and where anomalies are not blurred by lateral effects. Computation times are not discouraging and can probably be reduced further in the future.

Both the 1D and the 2D imaging procedures have an obvious potential for airborne and other continuous EM methods, where extremely large data sets require fast interpretation procedures. With the rapid development of such measuring strategies 3D interpretation of data from closely spaced profile lines is coming within reach. The above results indicate that there is reason to believe that 3D AIM procedures would also benefit from the use of the AB approximation.

Besides offering a fast method of getting a model section from measured data the full potential of the AB inverse lies in its application in an iterative AIM inversion. Fast forward algorithms for 2D TEM responses can be developed using the extended Born approximation (Habashy et al. 1993; Slob and van den Berg 1995) and the combination of a (sufficiently) exact forward modeling routine with the AB inverse should have a large potential as a final processing tool for profile oriented TEM measurements.

The one-pass 1D and 2D algorithms presented here have two weaknesses: 1) it is necessary to compute the step response from the convolved impulse response, and 2) from the step response the apparent conductivity must be determined. The transformation to step response is not an unconditionally stable procedure and it depends to a large extent – too large extent – on the parametrization of the step response. Furthermore, the determination of apparent conductivity from the step response is only unique for certain simple measuring configurations (central loop, coincident loop) or for certain intervals of time and conductivity. Both of these limitations are unsatisfactory, but there are ways to overcome these difficulties by avoiding the two processing steps mentioned above, so that the imaging procedures can be used for any configuration and for any transmitter waveform. The price paid for this is that the inversion becomes iterative and no longer one-pass. For the 1D case this is of no importance, as the processing will be extremely fast anyway, but the consequencies for the 2D case could be more severe. However, the step responses needed for the fast one-pass 2D algorithm could be found as model responses of

the imaged 1D models. This discussion shall not be carried any further here as it would be beyond the scope of this paper.

Based on the presented preliminary results it is concluded that the AB approximation is superior to the simple Born approximation. However, a systematic comparison of results obtained with the AB Born approximation and the extended Born approximation of Habashy et al. (1993) and the inverse procedures derived from it (Torres-Verdín and Habashy 1994, 1995) would be very interesting. The adaptive Born approximation offers an intermediate step between the simple Born and the extended Born approximations, which is as simple and fast to implement as the simple Born approximation.

Acknowledgements

This paper would not have been possible without the support from many people. If I have not already expressed my thanks let it be done here. However, I shall specifically mention a few. I am indebted to Esben Auken, Danish Technical University, for calculation of the 2D TEM model responses and to Torleif Dahlin, Lund Technical University, Sweden, for allowing me to use the Hallandsåsen data. Two anonymous reviewers offered constructive criticism which made this a better paper. I wish to thank professor Frank Morrison and Dr. Ki Ha Lee for discussions during my stay at Department of Minerals Sciences and Mining Engineering at University of California, Berkeley, and I appreciate the comments and suggestions received from Dr. F.J. Esparza. I am especially grateful for the inspiring discussions with Dough Oldenburg, University of British Columbia, and his encouragement.

References

Alumbaugh, D.L., Newman, G.A., Prevost, L., and Shadid, J.N.: 1995, 'Three dimensional wide band electromagnetic modeling on massively parallel computers', Submitted to *Radio Science*.

Anderson, W.L.: 1979, 'Computer program. Numerical integration of related Hankel transforms of orders 0 and 1 by adaptive digital filtering', *Geophysics* **44**(7), 1287–1305.

Anderson, W.L.: 1989, 'A hybrid fast Hankel transform algorithm for electromagnetic modeling', *Geophysics* **54**, 263–266.

Anderson, W.L.: 1995, 'Q-factor approximation of electromagnetic fields for high-frequency sounding in the 300 kHz to 30 MHz range over layered media', *Geophysics* **60**, 1253–1258.

Becker, A. and Cheng, G: 1987, 'Detection of repetitive electromagnetic signals', in M.N. Nabighian (ed.), *Electromagnetic Methods in Applied Geophysics*, Vol. 1, pp. 443–467, Investigations in Geophysics no. 3, Society of Exploration Geophysicists, P.O. Box 702740, Tulsa, Oklahoma 74170-2740.

Berenger, J.: 1993, 'A perfectly matched layer for the absorption of electromagnetic waves', *J. Comp. Phys.* **114**, 185–200.

Boerner, D.E. and West, G.F.: 1989, 'A generalized representation of the electromagnetic fields in a layered earth', *Geophysical Journal* **97**, 529–547.

Chave, A.D.: 1984, 'The Fréchet derivatives of electromagnetic induction', *J. Geophys. Res.* **89**(B5), 3373–3380.

Christensen, N.B.: 1990, 'Optimized fast Hankel transform filters', *Geophys. Prosp.* **38**, 545–568.

Christensen, N.B. and Auken, E.: 1992, 'Simultaneous electromagnetic layered model analysis', in B.H. Jacobsen (ed.), *Proceedings of the Interdisciplinary Inversion Workshop 1*, Aarhus 1992, GeoSkrifter 41, pp. 49–56.

Christensen, N.B. and Sørensen, K.I.: 1994, 'Integrated use of electromagnetic methods for hydrogeological investigations', *Proceedings of the Symposium on the Application of Geophysics to Engineering and Environmental Problems (SAGEEP)*, Boston, March 1994, pp. 163–176, Environmental and Engineering Geophysical Society, P.O. Box 4475, Englewood, CO 80155, USA.

Christensen, N.B.: 1995, 'Imaging of central loop transient electromagnetic soundings', *Journal of Environmental and Engineering Geophysics*, **0**(1), 53–66.

Christensen, N.B.: 1996, 'Imaging of transient electromagnetic soundings using a scaled Fréchet derivative', in B.H. Jacobsen, K. Mosegaard, and P. Sibani (ed.), *Inverse Methods. Interdisciplinary Elements of Methodology, Computation and Applications*, Lecture Notes in Earth Sciences, vol. 63, Springer-Verlag, Berlin-Heidelberg, ISSN 0930-0317, ISBN 3-540-61693-4.

Christensen, N.B. and Sørensen, K.I.: 1996, 'New strategies for surface and borehole electromagnetic methods in hydrogeophysical investigations', *European Journal of Environmental and Engineering Geophysics*, in review.

Dam, D., Christensen, N.B., and Sørensen, K.I.: 1996, 'Inversion of transient hydraulic head variation caused by a controlled point source', in B.H. Jacobsen, K. Mosegaard, and P. Sibani (ed.), *Inverse Methods. Interdisciplinary Elements of Methodology, Computation and Applications*, Lecture Notes in Earth Sciences, vol. 63, Springer-Verlag, Berlin-Heidelberg, ISSN 0930-0317, ISBN 3-540-61693-4.

Eaton, P.A. and Hohmann, G.W.: 1987, 'An evaluation of electromagnetic methods in the presence of geologic noise', *Geophysics* **52**, 1106–1126.

Eaton, P.A. and Hohmann, G.W.: 1989, 'A rapid inversion technique for transient electromagnetic soundings', *Phys. Earth Plan. Int.* **53**, 384–404.

Effersø, F. and Sørensen, K.I.: 1996, 'A new approach to in situ determination of the hydraulic conductivity', *Proceedings of the Symposium on the Application of Geophysics to Engineering and Environmental Problems (SAGEEP)*, Keystone, Colorado, pp. 1107–1113, Environmental and Engineering Geophysical Society.

Ellis, R.G. and Oldenburg, D.W.: 1994, 'Applied geophysical inversion', *Geophys. J. Int.* **116**, 5–11.

Esparza, F.J., Peres-Flores, M.A., Gallardo, L.A., and Gómez-Treviño, E.: 1993, 'A simple method of magnetotelluric inversion in two dimensions', *3rd International Congress of the Brazilian Geophysical Society*, Expanded abstracts, vol. 2, pp. 1461–1463.

Esparza, F.J., Gómez-Treviño, E., Rodrigues, U., and Romo, J.M..: 1996, 'A generalized Niblett-Bostick transformation for two-dimensional magnetotelluric inversion', *13th Workshop on Electromagnetic Induction in the Earth*, Onuma, Japan July 12–18 1996, pp. 69–70.

Gómez-Treviño, E.: 1987a, 'A simple sensitivity analysis of time-domain and frequency-domain electromagnetic measurements', *Geophysics* **52**, 10, 1418–1423.

Gómez-Treviño, E.: 1987b, 'Nonlinear integral equations for electromagnetic inverse problems', *Geophysics* **52**, 1297–1302.

Gómez-Treviño, E., Esparza, F.J., Perez-Flores, M.A., Flores, C., and Romo, J.M.: 1994, 'A simple magnetotelluric imaging method and its application to data from geothermal areas', *Proceedings of the XIIth Workshop of Electromagnetic Induction in the Earth*, Brest, August 1994.

Habashy, T.M., Groom, R.W., and Spies, B.R.: 1993, 'Beyond the Born and Rytov approximations: a nonlinear approach to electromagnetic scattering', *J. Geophys. Res.* **98**(B2), 1759–1775.

Haber, E. and Oldenburg, D.: 1996, 'Regularization and incomplete conjugate gradient', University of British Columbia, Vancouver, Canada.

Hanke, M., and Hansen, J.C.: 1993, 'Regularization methods for large scale problems', *Surveys on Mathematics for Industry*, **3**, 253–315.

Hanneson, J.E. and West, G.F.: 1984a, 'The horizontal loop electromagnetic response of a thin plate in a conductive earth: Part I Computational method', *Geophysics* **49**, 411–420.

Hanneson, J.E. and West, G.F.: 1984b, 'The horizontal loop electromagnetic response of a thin plate in a conductive earth: Part II Computational results and examples', *Geophysics* **49**, 421–432.

Hansen, P.C.: 1992, 'Numerical tools for analysis and solution of Fredholm integral equation of the first order', *Inverse Problems* **8**, 849–872.

Hohmann, G.W.: 1975, 'Three-dimensional induced polarization and electromagnetic modeling', *Geophysics* **40**, 309–324.

Hohmann, G.W. and Raiche, A.P.: 1987, 'Inversion of controlled-source electromagnetic data', in M.N. Nabighian (ed.), *Electromagnetic Methods in Applied Geophysics*, Vol. 1, pp. 469–503, Investigations in Geophysics no. 3, Society of Exploration Geophysicists, P.O. Box 702740, Tulsa, Oklahoma 74170-2740.

Hohmann, G.W.: 1987, 'Numerical modeling for electromagnetic methods in geophysics', in M.N. Nabighian (ed.), *Electromagnetic Methods in Applied Geophysics*, Vol. 1, pp. 313–363, Investigations in Geophysics no. 3, Society of Exploration Geophysicists, P.O. Box 702740, Tulsa, Oklahoma 74170-2740.

Jackson, D.D.: 1972, 'Interpretation of inaccurate, insufficient, and inconsistent data', *Geophys. J. R. Astr. Soc.* **28**, 97–109.

Jacobsen, B.H.: 1993, 'Practical methods of a priori covariance specification for geophysical inversion', in K. Mosegaard (ed.), *Proceedings of the Interdisciplinary Inversion Workshop 2*, Copenhagen.

Jacobsen, B.H.: 1996, 'Rapid 2D inversion by multichannel deconvolution of geophysical profile data', *Proceedings of the Symposium on the Application of Geophysics to Engineering and Environmental Problems (SAGEEP)*, Keystone, Colorado: 1996, pp. 659–668, Environmental and Engineering Geophysical Society.

Johansen, H.K., and Sørensen, K.I.: 1979, Fast Hankel Transforms, *Geophys. Prosp.* **27**, 876–901.

Lee, S., Lee, K.H., and Morrison, H.F.: 1990, 'Modeling of 3-D electromagnetic responses using a t-k method', *10th Workshop on Electromagnetic Induction in the Earth*, Encenada, B.C., Mexico.

Lee, K.H. and Xie G.: 1995, 'Finite element 3-D electromagnetic modeling', *Progress in Electromagnetic Research Symposium, Proceedings 1995*, University of Washington.

Levy, G.M.: 1984, 'Correction of measured transient electromagnetic responses for finite transmitter turn-off duration', *Technical note TN-16, Geonics Limited.*

Li, Y., and Oldenburg, D.W.: 1994, 'Inversion of 3-D DC resistivity data using an approximate inverse mapping', *Geophys. J. Int.* **116**, 527–537.

Loke, M.H. and Barker, R.D.: 1995, 'Least-squares deconvolution of apparent resistivity pseudosections', *Geophysics* **60**, 1682–1690.

Loke, M.H. and Barker, R.D.: 1996, 'Rapid least-squares inversion of apparent resistivity pseudosections by a quasi-Newton method', *Geophys. Prosp.* **44**, 131–152.

Mackie, R.L. and Madden, T.R.: 1993a, 'Conjugate direction relaxation solutions for 3-D magnetotelluric modeling', *Geophysics* **58**, 1052–1057.

Mackie, R.L. and Madden, T.R.: 1993b, 'Three-dimensional magnetotelluric inversion using conjugate gradients', *Geophys. J. Int.* **115**, 215–229.

Mackie, R.L., Smith, J.T., and Madden, T.R.: 1994, 'Three-dimensional electromagnetic modeling using finite difference equations: The magnetotelluric example', *Radio Science* **29**, 923–935.

Macnae, J.C., Lamontagne, Y., and West, G.F.: 1984, 'Noise processing techniques for time-domain EM systems', *Geophysics* **49**, 934–948.

Macnae, J.C. and Lamontagne, Y.: 1987, 'Imaging quasi-layered conductive structures by simple processing of transient electromagnetic data', *Geophysics* **52**, 545–554.

Macnae, J.C., Smith, R.S., Polzer, B.D., Lamontagne, Y., and Klinkert, P.S.: 1991, 'Conductivity-depth imaging of airborne electromagnetic step-reponse data', *Geophysics* **56**, 102–114.

Madsen, K. and Nielsen, H.B.: 1993, 'A finite smoothing algorithm for linear L_1 estimation', *SIAM J. Optimization* **3**(2), 223–235.

McGillivray, P.R., Oldenburg, D.W., Ellis, R.G., and Habashy, T.M.: 1994, 'Calculation of sensitivities for the frequency-domain electromagnetic problem', *Geophys. J. Int.* **116**, 1-4.

Møller, I., Christensen, N.B., and Jacobsen, B.H.: 1996, 'Deconvolution of geophysical multioffset resistivity profile data', in B.H. Jacobsen, K. Mosegaard, and P. Sibani (ed.), *Inverse Methods. Interdisciplinary Elements of Methodology, Computation and Applications*, Lecture Notes in Earth Sciences, vol. 63, Springer-Verlag, Berlin-Heidelberg, ISSN 0930-0317, ISBN 3-540-61693-4.

Nekut, A.G.: 1987, Direct inversion of time-domain electromagnetic data, *Geophysics* **52**, 1431–1435.

Newman, G.A. and Alumbaugh, D.L.: 1995, '3-D wide band frequency electromagnetic modeling using staggered finite element difference on massively parallel architectures', *Progress in Electromagnetic Research Symposium, Proceedings 1995*, University of Washington.

Oldenburg, D.W.: 1990, 'Inversion of electromagnetic data: An overview of new techniques', *Surveys in Geophysics* **11**, 231–270.

Oldenburg, D.W. and Ellis, R.G.: 1991, 'Inversion of geophysical data using an approximate inverse mapping', *Geophys. J. Int.* **105**, 325–353.

Oldenburg, D.W., McGillivray, P.R., and Ellis, R.G.: 1993, 'Generalized subspace method for large-scale inverse problems', *Geophys. J. Int.* **114**, 12–20.

Oldenburg, D.W. and Ellis, R.G.: 1993, 'Efficient inversion of magnetotelluric data in two dimensions', *Phys. Earth Plan. Int.* **81**, 177–200.

Oldenburg, D.W.: 1994, 'Practical strategies for the solution of large-scale electromagnetic inverse problems', *Radio Science* **29**(4), 1081–1099.

Oldenburg, D.W. and Li, Y.: 1994, 'Subspace linear inverse method', *Inverse Problems* **10**, 915–935.

Polzer, B.D.: 1985, 'The interpretation of inductive transient magnetic sounding data', *Research in Applied Geophysics*, No. 36, Geophysics Laboratory, Department of Physics, University of Toronto.

Pellerin, L., Labson, V.F., Pfeifer, M. C., and others: 1994, 'VETEM – a very early time electromagnetic system', *Proceedings of the Symposium on the Application of Geophysics to Engineering and Environmental Problems (SAGEEP)*, Boston, Massachusetts, pp. 795–802, Environmental and Engineering Geophysical Society, P.O. Box 4475, Englewood, CO 80155, USA.

Pellerin, L., Labson, V.F., Pfeifer, M. C., and others: 1995, 'VETEM – a very early time electromagnetic system – the first year', *Proceedings of the Symposium on the Application of Geophysics to Engineering and Environmental Problems (SAGEEP)*, Orlando, Florida, pp. 725–731, Environmental and Engineering Geophysical Society, P.O. Box 4475, Englewood, CO 80155, USA.

Qian, W. and Boerner, D.E.: 1995, 'Basis functions in 1D EM integral equation modeling', *International symposium on three-dimensional electromagnetics, Proceedings volume*, Schlumberger-Doll Research, Connecticut.

Raiche, A.: 1974, 'An integral equation approach to 3D modeling', *Geophys. J. Astr. Soc.* **36**, 363–376.

Raiche, A.: 1994, 'Modeling and inversion, progress, problems, and challenges', *Surveys of Geophysics* **15**, 159–208.

Slob, E.C. and van den Berg, P.M.: 1995, 'A new integral equation method for solving transient diffusive electromagnetic scattering problems', *International Symposium on Three-Dimensional Electromagnetics, Proceedings Volume*, Schlumberger-Doll Research, Connecticut.

Smith, R.S., Edwards, R.N., and Buselli, G.: 1994, 'An automatic technique for presentation of coincident-loop, impulse-response, transient, electromagnetic data', *Geophysics* **59**, 1542–1550.

Smith, R. and Paine, J.: 1995, '3D TEM modeling - a users' view', *International Symposium on Three-Dimensional Electromagnetics, Proceedings Volume*, Schlumberger-Doll Research, Connecticut.

Spies, B.R. and Eggers, D.E.: 1986, 'The use and misuse of apparent resistivity in electromagnetic methods', *Geophysics* **51**, 1462–1471.

Stewart, D. C., Anderson, W. L., Grover, T. P. and Labson, V. F.: 1994, 'Shallow subsurface mapping by electromagnetic sounding in the 300 kHz to 30 MHz range: Model studies and prototype system assessment', *Geophysics* **59**, 1201–1210.

Sørensen, K.I.: 1989, 'A method for measurement of the electrical formation resistivity while auger drilling', *First Break* **7**(10), 403–407.

Sørensen, K.I.: 1994, 'The Ellog auger drilling method', *Proceedings of the Symposium on the Application of Geophysics to Engineering and Environmental Problems (SAGEEP)*, March 1994, Boston, Massachusetts, pp. 985–994, Environmental and Engineering Geophysical Society, P.O. Box 4475, Englewood, CO 80155, USA.

Sørensen, K.I. and Christensen, N.B.: 1994, 'The fields from a finite electrical dipole – A new computational approach', *Geophysics* **59**, 864–880.

Sørensen, K.I. and Effersø, F.: 1995, 'Continuous transient electromagnetic sounding', *1st Meeting of the EEGS European Section*, Torino, Italy, pp. 472–475, Environmental and Engineering Geophysical Society, European section. P.O. Box 51, CH-1015 Lausanne, Switzerland.

Sørensen, K.I. and Sørensen, K.M.: 1995, 'Pulled array continuous vertical electrical sounding, PA-CVES', *Proceedings of the Symposium on the Application of Geophysics to Engineering and Environmental Problems*, April 1995, Orlando, Florida, pp. 893–898, Environmental and Engineering Geophysical Society, P.O. Box 4475, Englewood, CO 80155, USA.

Sørensen, K.I.: 1996a, 'Pulled array continuous electrical profiling', *First Break* **14**(3), 85–90.

Sørensen, K.I: 1996b, 'Dense spacial electromagnetic and electrical soundings in ground water investigations', *European Journal of Environmental and Engineering Geophysics*, in review.

Tarantola, A.: 1987, *Inverse Problem Theory*, Elsevier Science Publishers B.V.

Torres-Verdín, C. and Habashy, T.M.: 1994, 'Rapid 2.5-dimensional forward modeling and inversion via a new nonlinear scattering approximation', *Radio Science* **29**(4), 1051–1079.

Torres-Verdín, C. and Habashy, T.M.: 1995, 'A two-step linear inversion of two-dimensional electric conductivity', *IEEE Trans. Ant. Prop.* **43**(4), 405–415.

Walker, P.W. and West, G.F.: 1991, 'A robust integral equation solution for electromagnetic scattering by a thin plate in conductive media', *Geophysics* **56**, 1140–1152.

Wang, T. and Hohmann, G.W.: 1993, 'A finite-difference time-domain solution for three-dimensional electromagnetic modeling', *Geophysics* **58**, 797–809.

Wang, T. and Tripp, A.C.: 1994, 'FDTD simulation of EM wave propagation in 3-D media', submitted to *Geophysics*.

Wannamaker, P.E.: 1991, 'Advances in three-dimensional magnetotelluric modeling using integral equations', *Geophysics* **56**, 1716–1728.

Ward, S.H., and Hohmann, G.W.: 1987, 'Electromagnetic theory for geophysical applications', in M.N. Nabighian (ed.), *Electromagnetic Methods in Applied Geophysics*, Vol. 1, pp. 131–312, Investigations in Geophysics no. 3, Society of Exploration Geophysicists, P.O. Box 702740, Tulsa, Oklahoma 74170-2740.

Weidelt, P.: 1975, 'Electromagnetic induction in three-dimensional structures', *J. Geophys.* **41**, 85–109.

Whittall, K.P. and Oldenburg, D.W.: 1992, 'Inversion of magnetotelluric data over a one-dimensional conductivity', in D.V. Fitterman (ed.), *Geophys. Monogr. Ser.* **5**, Soc. of Explor. Geophys., Tulsa, Oklahoma.

Zhdanov, M.S. and Fang, S.: 1996, 'Quasi-linear approximation in 3-D electromagnetic modeling', *Geophysics* **61**, 646–665.